A PHYSICS-INFORMED NEURAL NETWORK FOR COUPLED CALCIUM DYNAMICS IN A CABLE NEURON

Zachary M. Miksis* **and Gillian Queisser†**
Department of Mathematics
Temple University
Philadelphia, PA 19122

ABSTRACT

Transcranial magnetic stimulation (TMS) is a noninvasive treatment for a variety of neurological and neuropsychiatric disorders by triggering a calcium response through magnetic stimulation. To understand the full effects of this treatment, researchers will often use numerical simulations to model and study the calcium response. These simulations are limited to short-time simulations of single neurons due to computational complexity, restricting their use in clinical settings. In this paper, we explore an application of physics-informed neural networks (PINNs) to accurately produce long-time simulations of neuronal responses, opening the possibility of utilizing these methods in clinical applications to directly benefit patients.

1 Introduction

Transcranial magnetic stimulation (TMS) is an invaluable tool for treating a variety of neurological and neuropsychiatric disorders in a noninvasive way by using a time-varying magnetic field passed through the brain to stimulate neurons (2; 7). This stimulation triggers a response from intracellular calcium, which is vital to regulating the transfer of information from synaptic sites to the cell nucleus (4). Ultimately, this allows for treatment of various forms of degenerative neurological disorders, and TMS is therefore used extensively in both research and clinical settings (8).

While TMS is very important, its full effects are still not entirely understood. To investigate these effects, computational tools and studies are exceptionally important to complement experimental studies (5). To this end, different numerical computation tools have been developed (3; 13; 6). While these tools are very good at capturing fine grain details and the quick responses to fast TMS frequencies, they are limited to short simulated time spans of single neurons due to computational complexity. In order to address these limitations, we look to neural networks (from here on, "neuron" will be used to refer to a biological neuron, and "neural network" will be used to refer to the machine learning paradigm).

Neural networks have been used in various applications, many focusing on image recognition and reconstruction (e.g., see (1)). More recently, knowledge of physical models have been introduced into neural networks to form physics-informed neural networks (PINNs) (11; 9; 10). In this work, we utilize these PINNs to incorporate partial differential equations (PDEs) that model calcium dynamics in neurons into the larger neural network. With a network that satisfies physical laws, we can build simulations that provide long-time results, overcoming one of the limitations of traditional numerical methods. This leads to another limitation of PINNs, in that they have been shown to have difficulty accurately to simulate diffusion problems (12). This can be overcome with strategies of both relaxation of the loss function and periodic activation functions (15; 14), which we utilize in our application.

This paper is structured as follows: In Section 2, we describe the physical model of calcium dynamics that is used (with further details in Appendix A). In Section 3, we describe the details on PINNs as we used them in our application. In Section 4, we present results of a simulated cable neuron. In Section 5, we draw conclusions from our results and describe the broader impacts of this work.

*miksis@temple.edu
†queisser@temple.edu

International Conference on Scientific Computing and Machine Learning 2024 (SCML2024)

2 Calcium Dynamics

Within a neuron, ion dynamics are modeled by reaction-diffusion equations of the form

$$\frac{\partial u}{\partial t} = D\Delta u + R(u), \tag{1}$$

where u is an ion concentration, D is the diffusion coefficient, and $R(u)$ is a reaction term. From Fick's first law, we have

$$J = -D\frac{\partial u}{\partial x}, \tag{2}$$

where J is the diffusion flux. This leads to the Neumann boundary condition

$$\frac{\partial u}{\partial x} = -\frac{J}{D}. \tag{3}$$

In the cytosol, the non-organelle interior of a neuron, calcium is transported via various mechanisms and is buffered by the molecule calbindin. We model this using a dimension-reduced system (4), given by

$$\frac{\partial c}{\partial t} = \nabla \cdot (D_c \nabla c_c) + f(b, c_c) + J_{PM}, \tag{4}$$

$$\frac{\partial b}{\partial t} = \nabla \cdot (D_b \nabla b) + f(b, c_c), \tag{5}$$

where the reaction term

$$f(b, c_c) = k_b^-(b^{tot} - b) - k_b^+ b c_c$$

models the reaction equation

$$\mathrm{Ca}^{2+} + \mathrm{CalB} \underset{\kappa_b^+}{\overset{\kappa_b^-}{\rightleftharpoons}} \mathrm{CalBCa}^{2+}, \tag{6}$$

and J_{PM} represents the net Ca^{2+} ion flux across the plasma membrane (separating intra- and extracellular space). This term can be broken down into the different mechanisms that transport calcium across the plasma membrane,

$$J_{PM} = -J_P - J_N + J_{SYN} + J_{VDCC}, \tag{7}$$

where J_P is the flux from plasma membrane Ca^{2+}-ATPase pumps (PMCA), J_N is the flux from Na^+/Ca^{2+} exchangers (NCX), J_{SYN} is the flux through the post-synaptic density (PSD), and J_{VDCC} is the flux from voltage dependent calcium channels (VDCCs). Details of how each flux term is calculated are given in Appendix A.

3 Physics-Informed Neural Networks

To simulate calcium dynamcis, we incorporate the above diffusion model into a physics-informed neural network (PINN) (11; 9; 10). Consider a general partial differential equation of the form

$$u_t + \mathcal{N}[u] = 0, \tag{8}$$

with $x \in \Omega$, $t \in [0, T]$, where $u(x, t)$ is the latent solution, $\mathcal{N}[\cdot]$ is a nonlinear differential operator, and Ω is the computational domain. Define $f(x, t)$ as the left-hand-side of Eq. (8),

$$f := u_t + \mathcal{N}[u]. \tag{9}$$

By approximating $u(x, t)$ using a deep neural network, we build a physics-informed neural network $f(x, t)$ by combining this network with Eq. (9). The shared terms of the networks are learned by minimizing the mean squared error loss

$$MSE = (1 - \alpha)MSE_u + \alpha(MSE_f + MSE_b), \tag{10}$$

where

$$MSE_u = \frac{1}{N_u}\sum_{i=1}^{N_u} |u(t_u^i, x_u^i) - u^i|^2 \tag{11}$$

represents the error of the initial condition,

$$MSE_f = \frac{1}{N_f}\sum_{i=1}^{N_f} |f(t_f^i, x_f^i)|^2 \tag{12}$$

represents the error of the operator f inside the domain, and

$$MSE_b = \frac{1}{N_b}\sum_{i=1}^{N_b} |u_x(t_b^i, x_b^i) + J/D|^2 \tag{13}$$

represents the error of the Neumann boundary conditions. Here, $\{t_u^i, x_u^i, u^i\}_{i=1}^{N_u}$ represents the initial condition training data, $\{t_f^i, x_f^i\}_{i=1}^{N_f}$ represents the collocation points within the domain (excluding the boundaries), and $\{t_b^i, x_b^i\}_{i=1}^{N_b}$ represents the boundary collocation points. In our minimization, we apply a relaxation parameter $\alpha \in (0, 1]$. This is selected *a priori* by trial and error, and may require tuning to fit a particular model (15).

A defining feature of the calcium model is that it is a pure diffusion problem, which have been difficult to accurately model with neural networks. PINNs were initally introduced with `tanh` activation function, and were demonstrated to perform well for advection-dominated problems (11). The *SIREN* network introduced the use of periodic activation functions (14), which have been demonstrated to correct for problems in modeling diffusion-dominated problems (12). Therefore, we utilize a `sin` activation function in our network to provide consistent long-time modeling.

4 Results

In this section, we demonstrate the effectiveness of PINNs in modeling calcium dynamics. All constants used are given in Table 1 and Table 2. We consider the computational domain $(x, t) : [-1, 1] \times [0, 1]$, and use a numerically computed solution as the exact solution (see (3) for details on numerical methods). This is effectively a short time simulation that is not difficult to numerically simulate, but a learned model may be used for long time simulations (100 to 1000 times longer). The network consists of 4 hidden layers of 50 computational neurons each. The network is initialized with a uniform *Xavier* scheme, and

an *Adam* optimizer with learning rate of 0.001 is used to minimize the MSE. $N = 300$ collocation points are randomly generated on both the interior of the domain and the boundary (50 on each spatial boundary and 50 on the initial condition). These can be seen in Fig. 1.

For the biological model, we introduce a constant stimulus at the soma for the entire simulation time, and a constant voltage is applied. As can be seen in Appendix A, the gating function for VDCCs requires the solution of two ODEs. For the purposes of simulating TMS treatment protocols, predetermined voltage data may be provided to review its effects. Since the gating function only requires voltage and temporal values, these gating probabilities may be precomputed prior to training the network. We therefore avoid the requirement of modeling additional ODEs, and provide these gating probabilities explicitly to the network.

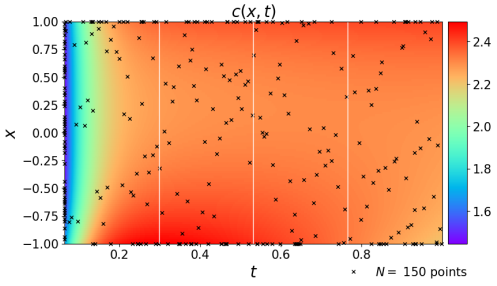

Figure 1: Domain collocation points

We first look at the values of the initial calcium and calbindin concentrations. In the numerical simulation, the initial concentrations are given as constant values. These may not represent the true steady state, and they will not satisfy the diffusion model, which leads to error in the PINN if they are used. We therefore consider the initial condition as the computed values after a small number of numerical timesteps ($\sim$5% of the total timesteps), as the concentrations are approaching values that satisfy the diffusion model. As the number of numerical timesteps is selected *a priori*, the values are still not guaranteed to be consistent with the diffusion model, but this significantly improves the performance of the PINN.

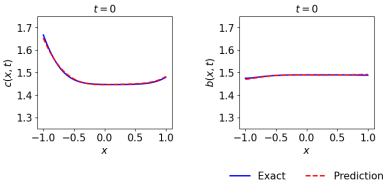

Figure 2: Initial concentrations

In Fig. 2, we show the results of the network prediction of the initial concentrations. While there is a small amount of error, we can see that the network fairly accurately predicts these values, with a numerical L^2 error in the calcium of 1.34×10^{-3}. In Fig. 4 and Fig. 5, we see that this error is significantly reduced to nearly vanishing as the simulation moves forward in time and the concentration values become consistent with the diffusion model. By the final time, the numerical L^2 error in the calcium has dropped to 5.83×10^{-4}.

For TMS treatment purposes, we may be interested in what is occurring at the soma (cell body) of the neuron. Fig 3 shows the concentration over time at the soma of our cable neuron. We see that the network very accurately predicts the concentrations of both calcium and calbindin over time, producing a solution nearly indistinguishable from the exact solution.

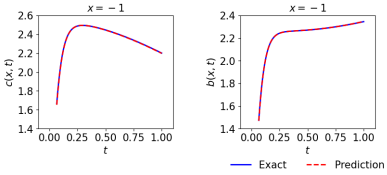

Figure 3: Concentrations at soma

5 Conclusions

In this study, we presented a physics-informed neural network (PINN) for modeling a coupled calcium model in a cable neuron. This is significant for the study of repetitive transcranial magnetic stimulation (rTMS), as it allows for long-time simulations with near instantaneous results. While traditional numerical methods provide accurate solutions, the requirement of small timesteps results in significant computation time and hampering the use for simulating a full rTMS treatment that could last several minutes with voltage pulses in millisecond bursts (13). Training a PINN on a short timespan allows for feeding data into the fully trained network and producing a long simulation.

Our results show that PINNs are capable of accurately capturing the calcium concentration over a cable neuron, which can be extended over time. While this work is limited to a single cable neuron, using this to create branches, and therefore a full neuron model, is an important direction for future work.

Broader Impact

Transcranial Magnetic Stimulation is an important noninvasive treatment for a wide array of neurological disorders. While the neuronal response to TMS is still poorly understood, simulation tools are providing a way of studying these effects and how they will benefit patients. A limiting factor in this research has been the difficulty in developing long-time simulations using traditional numerical methods. Neural networks provide the ability to provide long-time simulations with ease that may be applied in both a research and clinical setting, benefitting researchers and patients alike. Our work is an important step in that direction, and has the potential to fill this need.

Table 1: Values of constants in calcium model and fluxes

Constant	Value
D	1
b^{tot}	5
k_b^-	6
k_b^+	3
J_P	
ρ_P	2
I_P	1E-2
K_P	3
J_N	
ρ_N	2E5
I_N	1E-4
K_N	180
J_{SYN}	
j_{rls}	1

Table 2: Values of constants in calcium model VDCC flux

Constant	Value
J_{VDCC}	
R	8.314
F	96485
T	310
z	2
$\tau_{k,0}$	1.7E-3
$\tau_{l,0}$	70E-3
K_k	1.7E-3
K_l	70E-3
z_k	2
z_l	1
γ_k	0
γ_l	0
$V_{1/2,k}$	-21E-3
$V_{1/2,l}$	-40E-3

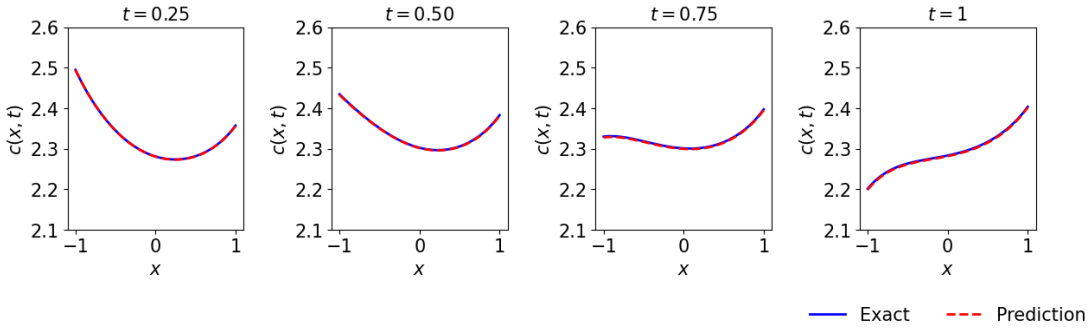

Figure 4: Calcium concentrations

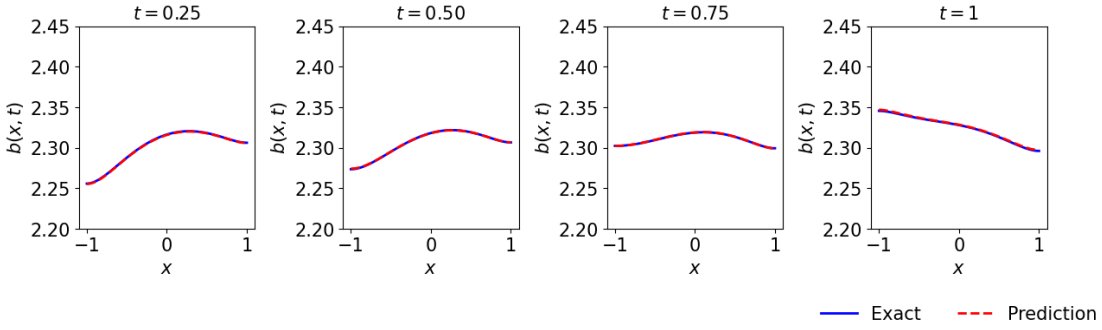

Figure 5: Calbindin concentrations

Acknowledgments

This work was supported by NIH grant R01EB034143.

References

[1] S. Abraham, J. Kinnison, Z. M. Miksis, D. Poster, S. You, J. D. Hauenstein, and W. Scheirer, *Efficient hyperparameter optimization for atr using homotopy parametrization*, in Automatic Target Recognition XXXIII, R. I. Hammoud, T. L. Overman, and A. Mahalanobis, eds., vol. 12521, 2023, p. 1252107.

[2] A. T. Barker, R. Jalinous, and I. L. Freeston, *Non-invasive magnetic stimulation of human motor cortex*, The Lancet, 325 (1985), pp. 1106–1007.

[3] P. Borole, *CalciumSim: Simulator for calcium dynamics on neuron graphs using dimensionally reduced model*, 2022.

[4] P. R. Borole, J. M. Rosado, M. Neal, and G. Queisser, *Neuronal resilience and calcium signaling pathways in the context of synapse loss and calcium leaks: A computational modeling study and implications for alzheimer's disease*, SIAM Journal on Applied Mathematics, 83 (2023), pp. 2418–2442.

[5] S. Grein, M. Stepniewski, S. Reiter, M. M. Knodel, and G. Queisser, *1d-3d hybrid modeling-from multi-compartment models to full resolution models in space and time*, Frontiers in Neuroinformatics, 8 (2014).

[6] Q. Guan and G. Queisser, *Modeling calcium dynamics in neurons with endoplasmic reticulum: Existence, uniqueness and an implicit–explicit finite element scheme*, Communications in Nonlinear Science and Numerical Simulation, 109 (2022), p. 106354.

[7] M. Hallett, *Transcranial magnetic stimulation: A primer*, Neuron, 55 (2007), pp. 187–199.

[8] J.-P. Lefaucheur, N. André-Obadia, A. Antal, S. S. Ayache, C. Baeken, D. H. Benninger, R. M. Cantello, M. Cincotta, M. de Carvalho, D. De Ridder, H. Devanne, V. Di Lazzaro, S. R. Filipović, F. C. Hummel, S. K. Jääskeläinen, V. K. Kimiskidis, G. Koch, B. Langguth, T. Nyffeler, A. Oliviero, F. Padberg, E. Poulet, S. Rossi, P. M. Rossini, J. C. Rothwell, C. Schönfeldt-Lecuona, H. R. Siebner, C. W. Slotema, C. J. Stagg, J. Valls-Sole, U. Ziemann, W. Paulus, and L. Garcia-Larrea, *Evidence-based guidelines on the therapeutic use of repetitive transcranial magnetic stimulation (rtms)*, Clinical Neurophysiology, 125 (2014), pp. 2150–2206.

[9] M. Raissi, P. Perdikaris, and G. E. Karniadakis, *Physics informed deep learning (part i): Data-driven solutions of nonlinear partial differential equations*, arXiv preprint arXiv:1711.10561, (2017).

[10] ——, *Physics informed deep learning (part ii): Data-driven discovery of nonlinear partial differential equations*, arXiv preprint arXiv:1711.10566, (2017).

[11] M. Raissi, P. Perdikaris, and G. E. Karniadakis, *Physics-informed neural networks: A deep learning framework for solving forward and inverse problems involving nonlinear partial differential equations*, Journal of Computational Physics, 378 (2019), pp. 686–707.

[12] M. H. Saadat, B. Gjorgiev, L. Das, and G. Sansavini, *Neural tangent kernel analysis of pinn for advection-diffusion equation*, arXiv preprint arXiv:2211.11716, (2022).

[13] S. Shirinpour, N. Hananeia, J. Rosado, H. Tran, C. Galanis, A. Vlachos, P. Jedlicka, G. Queisser, and A. Opitz, *Multi-scale modeling toolbox for single neuron and subcellular activity under transcranial magnetic stimulation*, Brain Stimulation, 14 (2021), pp. 1470–1482.

[14] V. Sitzmann, J. Martel, A. Bergman, D. Lindell, and G. Wetzstein, *Implicit neural representations with periodic activation functions*, in Advances in Neural Information Processing Systems, vol. 33, 2020, pp. 7462–7473.

[15] W. Snyder, I. Tezuar, and C. R. Wentland, *Domain decomposition-based coupling of physics-informed neural networks via the schwarz alternating method*, arXiv preprint arXiv:2311.00224, (2023).

Appendix A: Membrane Flux Components

The plasma membrane flux in this study can be separated as

$$J_{PM} = -J_P - J_N + J_{SYN} + J_{VDCC}. \tag{14}$$

In this section, we give a brief description of each component as described in (4).

PMCA Pumps A second-order Hill equation is used to model the plasma membrane Ca^{2+} current of PMCA pumps,

$$J_P(c_c) = \rho_P \cdot \frac{I_P c_c^2}{K_P^2 + c_c^2}, \tag{15}$$

where ρ_P is the density of PMCA pumps on the plasma membrane, I_P is the single channel Ca^{2+} current, c_c is the cytosolic Ca^{2+} concentration, and K_P is the measure of Ca^{2+} affinity.

NCX Exchangers A second-order Hill equation is used to model the plasma membrane Ca^{2+} current of NCX exchangers,

$$J_N(c_c) = \rho_N \cdot \frac{I_N c_c}{K_N + c_c} \tag{16}$$

where ρ_N is the density of NCX exchangers on the plasma membrane, I_N is the single channel Ca^{2+} current, c_c is the cytosolic Ca^{2+} concentration, and K_N is the measure of Ca^{2+} affinity.

Synaptic Influx Calcium influx is modeled by a linearly decreasing function:

$$J_{SYN} = j_{rls} \cdot \left(1 - \frac{t - t_0}{\tau_{rls}}\right) \lambda_{t_0}(t) \tag{17}$$

where j_{rls} is the current density and τ_{rls} is the associated time constant. The function $\lambda_{t_0}(t)$ is given by:

$$\lambda_{t_0}(t) = \begin{cases} 1, & t \in [t_0, t_0 + \tau_{rls}] \\ 0, & \text{otherwise.} \end{cases} \tag{18}$$

VDCCs For VDCCs, we use a Borg-Graham model. The Ca^{2+} current is given by

$$J_{VDCC}(V, c_c, t) = G(V, t) F(V, \Delta[Ca^{2+}]), \tag{19}$$

where $G(V, t) \in [0, 1]$ is the gating function and $F(V, \Delta[Ca^{2+}])$ is the flux function. The difference between cytoplasmic and extracellular ion concentration is given by

$$\Delta[Ca^{2+}] = c_c - c_o,$$

and the flux function is given by the Goldman-Hodgkin-Katz equation,

$$F(V, \Delta[Ca^{2+}]) = \overline{p}_{Ca^{2+}} \frac{V z^2 F^2}{RT} \cdot \frac{c_c - c_o \exp(-zFV/RT)}{1 - \exp(zFV/RT)} \tag{20}$$

where R is the universal gas constant, F is Faraday's constant, T is temperature in Kelvin, $\overline{p}_{Ca^{2+}}$ is the permeability of Ca^{2+} ions through the channels, and z is the valence of a Ca^{2+} ion. The gating function for N-type VDCCs is given by

$$G(V, t) = k(V, t) l^2(V, t), \tag{21}$$

where the gating functions $k(\cdot)$ and $l(\cdot)$ satisfy the two ODEs

$$\frac{\partial k}{\partial t} = \frac{k_\infty - k}{\tau_k} \quad \text{and} \quad \frac{\partial l}{\partial t} = \frac{l_\infty - l}{\tau_l},$$

where

$$k_\infty = \frac{\alpha_k(V)}{\alpha_k(V) + \beta_k(V)}; \qquad l_\infty = \frac{\alpha_l(V)}{\alpha_l(V) + \beta_l(V)},$$

and

$$\tau_k = \frac{1}{\alpha_k + \beta_k} + \tau_{k,0}; \qquad \tau_l = \frac{1}{\alpha_l + \beta_l} + \tau_{l,0}.$$

The rate functions are defined as

$$\alpha_k(V) = K_k \exp\left(\frac{z_k \gamma_k (V - V_{1/2,k}) F}{RT}\right)$$
$$\beta_k(V) = K_k \exp\left(\frac{-z_k (1 - \gamma_k)(V - V_{1/2,k}) F}{RT}\right)$$
$$\alpha_l(V) = K_l \exp\left(\frac{z_l \gamma_l (V - V_{1/2,l}) F}{RT}\right)$$
$$\beta_l(V) = K_l \exp\left(\frac{-z_l (1 - \gamma_l)(V - V_{1/2,l}) F}{RT}\right)$$